Dynamic scaling of hysteresis in a linearly driven system

1994 J. Phys.: Condens. Matter 6 7785

(http://iopscience.iop.org/0953-8984/6/38/016)

J. Phys.: Condens. Matter 6 (1994) 7785–7796. Printed in the UK

Dynamic scaling of hysteresis in a linearly driven system

F Zhong†, J X Zhang† and G G Siu‡

† Department of Physics, Zhongshan University, Guangzhou, People's Republic of China

‡ Department of Physics and Material Science, City Polytechnic of Hong Kong, Kowloon, Hong Kong

Received 1 March 1994, in final form 23 May 1994

Abstract. We investigate the scaling behaviour of hysteresis in three-dimensional continuum models in a linear driving mode. A non-conserving N-component vector Φ is the order parameter and its dynamics are specified by the time-dependent Ginzburg–Landau theory. The $(\Phi^2)^2$ and $(\Phi^2)^3$ models embody spatial fluctuations of Φ and their free-energy functionals have a $(\Phi^2)^2$ and a $(\Phi^2)^3$ interaction, respectively, with O(N) symmetry. On the other hand, the mean-field model ignores all spatial fluctuations of Φ. The area A of hysteresis loop, the energy dissipation per cycle, is taken as functions of the scanning rate R and temperature. For the ferromagnetic first-order phase transition (FOPT), a scaling relation $A = aR^n$ is determined where R is the field-sweeping rate, a is the coefficient and the exponent $n \simeq \frac{1}{2}$. We also discuss experimental evidence for real systems compatible with this result, which shows that the driving rate dependence of energy dissipation is important in non-equilibrium FOPT.

1. Introduction

Experimental and theoretical studies on the non-equilibrium dynamics of the first order phase transition (FOPT) show that there are general scaling behaviours in kinetics of ordering and spinodal decomposition. In the phase separation and grain growth of quenched alloys in a two-phase region (e.g. [1–3]), the ordering dynamics obey a power law $L \propto t^a$ for a phase approaching equilibrium from an initial non-equilibrium disorder state, where L is a characteristic length (e.g. the average ordered domain size) and t is the time. The exponent a depends only on related conservation laws and on universal parameters. This behaviour displays the scaling relations of the order-parameter correlation function and its Fourier transform, the structure factor [4]. The value of a can be determined based on the Binder–Stauffer [5] theory of cluster diffusion reaction and the Lifshitz–Slyozov [6] condensation theory. $a = \frac{1}{3}$ for low temperatures in a long time from the former theory [7], and for pure systems with a conserved order parameter but no hydrodynamic couplings by the latter theory [6]. $a = 1/(2 + d)$ for intermediate temperatures in an intermediate time [7, 8]. $a = \frac{1}{2}$ for a pure system with a non-conserved order parameter [9, 10].

Hysteresis is a common non-equilibrium phenomenon at the FOPT, which concerns metastable states and the dynamic behaviour of a drive system. In the thermoelastic martensitic transformation, uniformly increasing the loading induces a FOPT and then linear unloading reverses it [11]. A plot of stress σ as a function of strain ϵ yields a hysteresis superelastic loop. The stress hysteresis H, defined as the difference between the critical stresses of the forward and the reverse transformations, depends on the strain rate ($1/H \propto -\log \dot{\epsilon}$) and temperature ($H \propto 1/T$), implying scaling relations (figures 21 and 22 of [11]). The hysteresis of ferromagnetic materials, magnetic or thermal, was investigated

0953-8984/94/387785+12$19.50

on the basis of model systems [12, 13]. The loop area A was taken as the 'hysteresis'; $A \sim H_0^{0.66}\Omega^{0.33}$ where H_0 is the amplitude of the magnetic field and Ω the frequency of periodic driven field when both H and Ω are low. Scaling behaviour in hysteresis has thus been recognized. However, the driving mode, linear or sinusoidally periodic, determines the characteristic variable and the form of the scaling law.

Linear driving is commonly adopted, i.e. an external field varies uniformly with time. Linear heating or cooling in a differential scanning calorimeter and internal-friction pendulum, linear loading or unloading in thermoelastic martensitic transformation, and linear sweeping of magnetic field in electron spin resonance are several examples. The mechanical, thermal, electric or magnetic response or a driven system is investigated through their dependence on heating, loading or field-sweeping rate [14–19]. In studying the domain wall motion of magnetic materials, the internal friction was measured with different magnetic field-sweeping rates $\dot{H}$ and the total dissipated dynamic energy Q_v was shown to be proportional to $\dot{H}^s$ where s is an exponent parameter and $s < \frac{1}{2}$ for soft ferromagnetic materials such as Fe, Ni and Permalloy-42 [15, 16]. Similar relations appear in the plastic deformation of Al [18] and in the martensitic phase transition of Ni–Ti [19] where the heating rate $\dot{T}$ or the loading rate $\dot{e}$ serve as the natural measure of the driving. The scaling behaviour of dissipation in the FOPT is strongly suggested by experimental evidence of real systems which has recently emerged after extensive investigation, although the Steinmetz law, hysteresis dissipation $\propto B_m^{1.6}$, was published as early as in 1892 [12].

This work aims at describing the non-equilibrium statistical mechanics of a model system driven by a linearly varying external field in the FOPT. We study the response of the $(\Phi^2)^2$, $(\Phi^2)^3$ and mean-field models to linear field driving. The dependence of the area of hysteresis loops on the linear scanning rate R and its scaling relations are determined.

2. The $(\Phi^2)^2$ model

In the terminology of magnetism, the external driving force is the magnetic field H which increases or decreases linearly, and a hysteresis loop of magnetization M versus field H results from one cycle of field sweeping. The order parameter Φ is a N-component vector which is not conserved. The dynamics of Φ are described by the time-dependent Ginzburg–Landau theory and its equation of motion is

$$\frac{\partial \Phi}{\partial t} = -\Gamma \frac{\delta F}{\delta \Phi} + \eta \tag{1}$$

where Γ is the kinetic coefficient, a constant in the case of non-conserved order parameter, η is Gaussian white noise given by

$$\langle \eta(x, t) \rangle = 0 \tag{2}$$

$$\langle \eta_i(x, t)\eta_j(x, t) \rangle = 2\Gamma\delta_{ij}\delta(x - x')\delta(t - t') \tag{3}$$

F is the Landau–Ginzburg–Wilson free-energy functional given by

$$F(\Phi) = \tfrac{1}{2}\int \mathrm{d}^d x \left((\nabla\Phi)^2 + r\Phi^2 + \frac{u}{2N}(\Phi^2)^2 - 2\sqrt{N}H \cdot \Phi \right) \tag{4}$$

r is the temperature relative to the mean-field critical temperature, u is a parameter and H is the conjugate field of Φ. The uniform magnetic field H is taken along the direction of the first component of Φ.

The stochastic differential equation (1) in three-dimensional space, in the $N \to \infty$ limit, leads to the coupled integrodifferential equations [12, 20, 21]

$$\frac{dM}{dt} = \tfrac{1}{2}(a_\perp M + H) \tag{5a}$$

$$\frac{\partial C_i(q,t)}{\partial t} = 1 + (a_i - q^2)C_i(q,t) \tag{5b}$$

$$a_i = -(r + uS + uM^2 + 2uM^2\delta_{i1}) \tag{5c}$$

and

$$S = \frac{1}{2\pi^2}\int_0^1 q^2 C_\perp(q,t)\, dq. \tag{5d}$$

The magnetization M is given by $\langle\Phi(x,t)\rangle\,\delta_{i1}$, $C(q,t) = \langle\Phi(q,t)\cdot\Phi(-q,t)\rangle$ is the structure factor and $C_\perp$ is the transverse structure factor. The momentum cut-off is set to unity.

At $H = 0$, the equilibrium phase is readily obtained by dropping the time derivatives in equation (5). At a temperature $r > r_c = -u/[2\pi^2] = -S_c$,

$$M = 0,\ C_i(q) = 1/(q^2 - a_i).$$

At a temperature $r < r_c$

$$a_\perp = 0,\ C_\perp = 1/q^2,\ S = S_c \text{ and } M = \pm\sqrt{(r_c - r)/u}.$$

Consequently, when the system is quenched from a high-temperature paramagnetic phase to the ferromagnetic phase, it does not introduce any symmetry-breaking mechanism so that no magnetization results. The structure factor at later time can be well approximated [21] by

$$C(q,t) = C_{NG}(q,t) + D(q,t)$$

where $C_{NG}(q,t) = (1/q^2)[1 - \exp(-q^2 t)]$ relates the growth of Nambu–Goldstein modes and $D(q,t)$ describes the ordering development which can be put in a scaling form

$$D(q,t) = L^d(t)F[qL(t)]. \tag{6}$$

L is a characteristic length, d is the spatial dimension ($d = 3$ here) and F the scaling function: $L(t) \sim t^{1/2}$. The scaling of equation (6) can be checked by the average wavenumber

$$\bar{q} = \left(\frac{1}{2\pi^2}\int_0^1 q D(q,t) q^2\, dq\right) \Big/ \left(\frac{1}{2\pi^2}\int_0^1 D(q,t) q^2\, dq\right)$$

in a sufficiently long time, which gives $\bar{q} \sim L^{-1}(t)$.

We are interested in the system response to linear sweeping of an external field. The system will undergo an FOPT from a positive-magnetization phase to a negative-magnetization phase as the field reverses. The process is similar to nucleation since there is no sharp interface between these two phases when N is larger than unity. Equation (5), a set

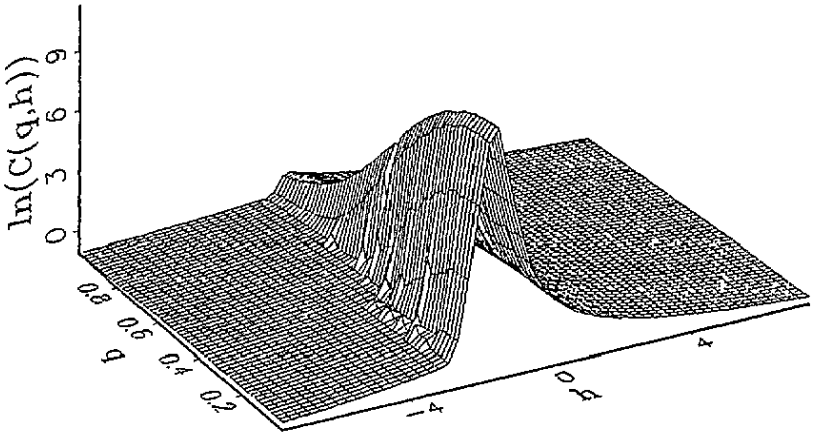

Figure 1. Structure factor C as a function of magnetic field H and wavenumber q.

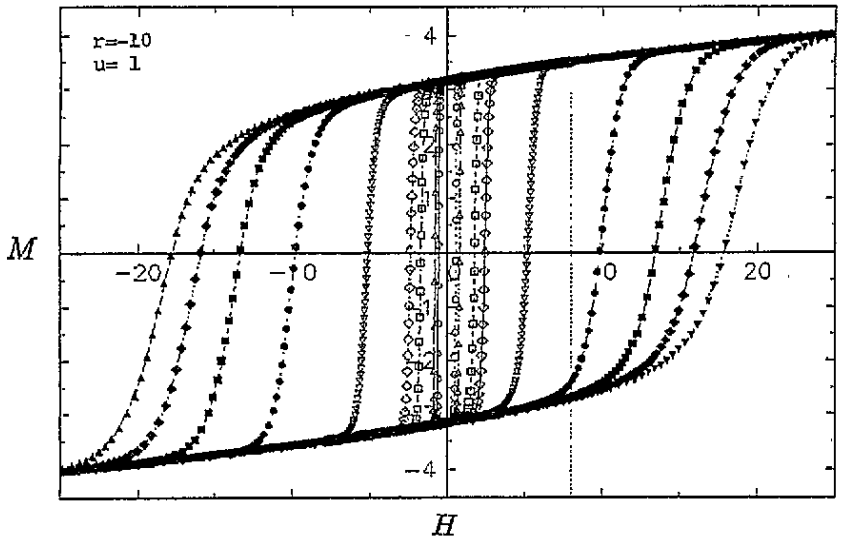

Figure 2. Hysteresis loop as a function of field-sweeping rate R at $r = -10$ and $u = 1$. R = 0.001, 0.005, 0.01, 0.05, 0.1, 0.5, 2, 4, 6, from the inside to the outside.

of non-linear integrodifferential equations, cannot be solved analytically for $H = Rt$. We use numerical computation: an adaptive-size Runge–Kutta scheme to solve the equations and a 20-point Gaussian quadrature to evaluate the integrals. The computer program is checked carefully while the scaling of the quenched structure factor also serves as a test. Given a temperature $r < r_c$, a parameter u and a scanning rate R, the field increases first to a definite value H_0, then decreases at a rate $-R$ to $-H_0$ and finally increases again to H_0 to complete the cycle. There is a limitation of R in computation; it will take too long to complete the cycle when $R \sim 2|r|$ (approximately equal to the relaxation rate in the quasi-equilibrium region) so that $R < 2|r|$ is chosen.

The results show that the magnetization M and structure factor C are independent of

the initial conditions. Figure 1 shows the surface of structure factor C versus field H and wavenumber q. The transverse structure factor $C_\perp$ reaches the maximum at $H = 0$ but, beyond a small range centred at 0, $C_\perp$ drops to nearly zero and is almost constant at a given H for different q. Figure 2 shows the sweeping rate dependence of the hysteresis loop, which expands horizontally and the saturation value increases slightly with the rate R. Figure 3 shows hysteresis loops at different temperatures. As r becomes more negative, i.e. the temperature becomes lower, the fluctuation in magnetization weakens and the loop 'grows' noticeably; both the remanence and the coercive force increase. The area A of the hysteresis loop, the dissipated energy per cycle, increases in both cases. Figure 4 shows the log A versus log R lines at different r, which are parallel to each other with the same slope n of about $\frac{1}{2}$. The data can be fitted to a scaling form

$$A = aR^n \tag{7}$$

(table 1). n tends to exactly $\frac{1}{2}$ as r becomes more negative. It is related to a property of the zero-temperature fixed point in quenched ordering [22]. The coefficient a can be fitted to $a_0(r_c - r)^m$, which gives $m = 0.87$ for $u = 1$, and $m = 0.84$ for $u = 10$. Figure 5 give the $A/(r_c - r)^m$ versus R lines ($v = 0$), both in logarithmic coordinates, and it shows that the dissipation scaling with linear scanning rate is applicable to different r and u.

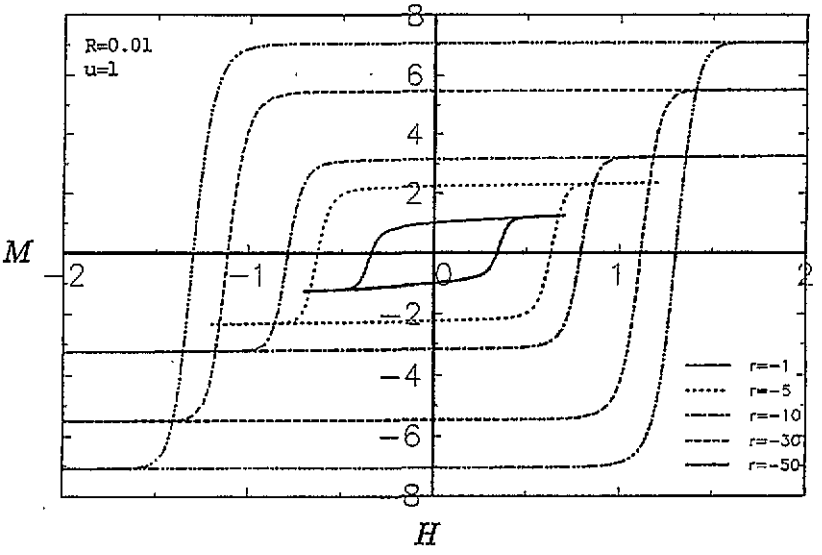

Figure 3. Hysteresis loop as a function of temperature r at $u = 1$ and $R = 0.01$. $r = -1, -5, -10, -30, -50$ from the inside to the outside.

Table 1. The fitted values of a and n in $A = aR^n$ (figure 4).

r	a	n
− 1.0	10.62	0.45
− 5.0	46.54	0.46
−10	89.90	0.48
−30	226.98	0.49
−50	345.19	0.49

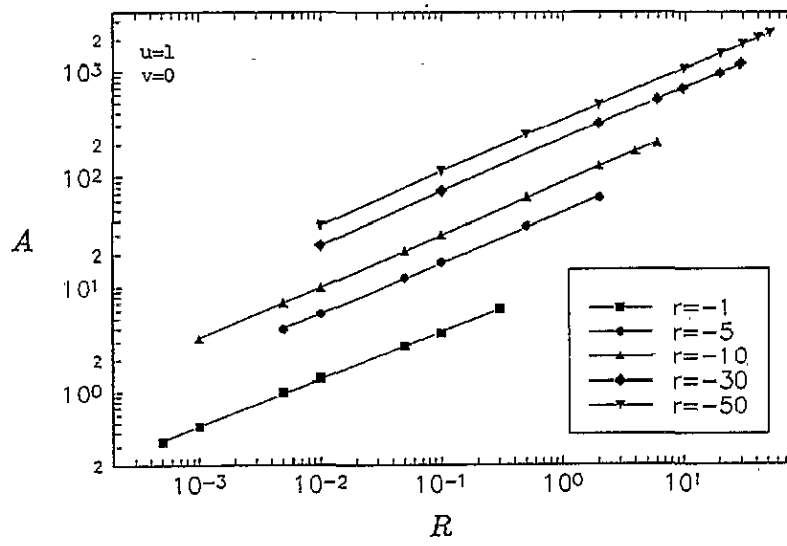

Figure 4. The lines of log A versus log R at different temperature ($u = 1$). $r = -1, -5, -10, -30, -50$ from the bottom to the top. They are parallel to each other with a slope almost equal to $\frac{1}{2}$ (table 1).

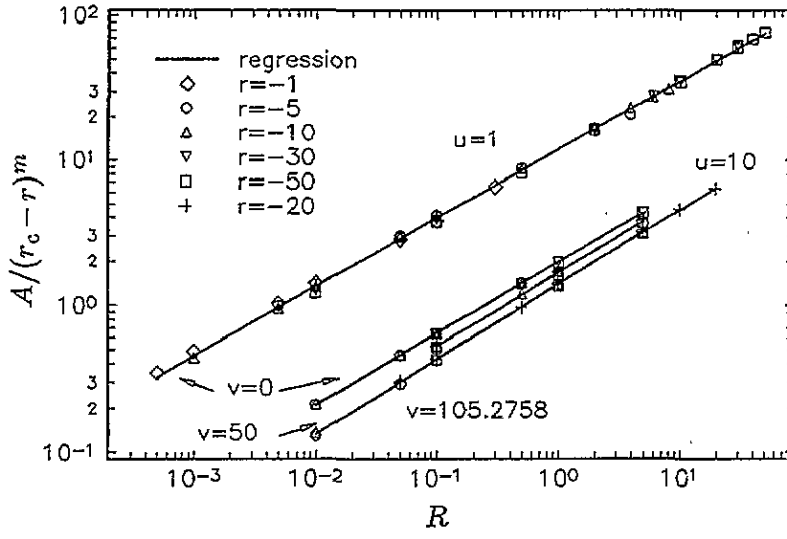

Figure 5. The lines of $\log[A/(r_c - r)^m]$ versus $\log R$. All data points in figure 4 at different temperatures now become the same line ($u = 1$), showing that the temperature dependence of the coefficient a has been taken into account. The $u = 10$ line is also plotted. These two lines are based on the $(\Phi^2)^2$ model ($v = 0$). Another two lines are based on the $(\Phi^2)^3$ model at $u = 10$, $v = 50$ and 105.2758, for hysteresis loops on the side of the second-order phase boundary in ferromagnetic region.

3. The $(\Phi^2)^3$ model

We extend our analysis of hysteresis to the three-dimensional $(\Phi^2)^3$ model whose free-energy functional includes a $(\Phi^2)^3$ term with O(N) symmetry:

$$F(\Phi) = \tfrac{1}{2}\int \mathrm{d}^d x\left((\nabla\Phi)^2 + r\Phi^2 + \frac{u}{2N}(\Phi^2)^2 + \frac{v}{3N^2}(\Phi^2)^3 - 2\sqrt{N}H\cdot\Phi\right) \tag{8}$$

with a new parameter v. The order parameter is non-conserved in quenched ordering [23] and it displays hysteresis in periodic driving [13]. In the limit of $N \to \infty$, its dynamics obey the same equation (5) except now

$$a_i = -\left(r + uS + uM^2 + vM^4 + 2vM^2S + vS^2\right). \tag{5c}$$

A paramagnetic phase and a ferromagnetic phase separated by a phase transition curve at $H = 0$ (the r–u plane) exits. This phase boundary divides into first-order 'half' and second-order 'half' by a tricritical point if $0 < v < v_c = 16\pi^2$ (the first-order boundary will develop two first-order wings on either side of the $H = 0$ plane when H is applied). For $v > v_c$, two halves meet at a critical end point and the first-order curve then extends to an ordinary critical point [24]. For comparison, we investigate only the case $v < v_c$ as in [13]. When $H \neq 0$, reversing the field will induce the FOPT from one direction of magnetization (up or down) to another when the system is initially at equilibrium in the ferromagnetic phase, or from the paramagnetic phase to the ferromagnetic phase when the system is initially in the paramagnetic phase in the first-order region so that a double hysteresis loop results. Furthermore, the model also exhibits a temperature-induced FOPT which we leave for further study.

At $H = 0$, a temperature drop changes the system from an initial disordered phase to the ferromagnetic phase in both the second- and the first-order regions. Figure 6 shows the $\bar{q}^{-1}$ versus t curve with different parameters including the $(\Phi^2)^2$ model ($v = 0$). At a long time, all data points lie on the same curve. It shows that the $\frac{1}{2}$ growth law is universal and confirms our computation.

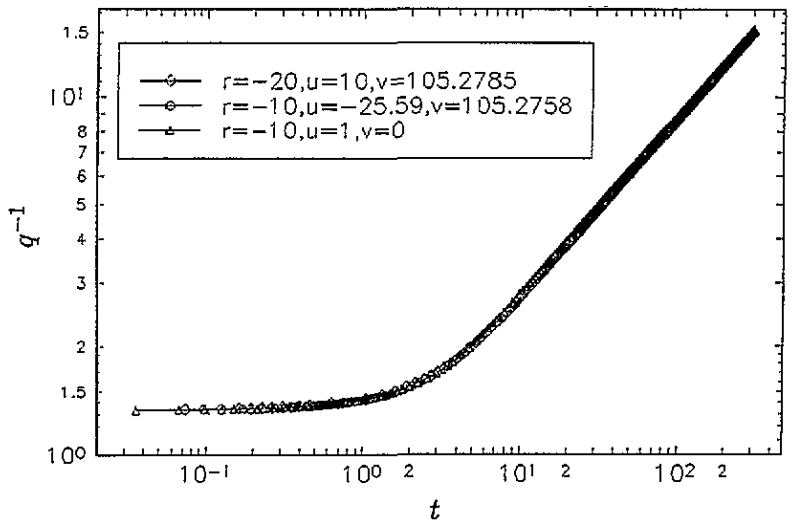

Figure 6. The $\bar{q}^{-1}$ versus t curve. The curve 'thickens' owing to overlapping of data points.

We obtain the area A of hysteresis loop by a computation similar to that in section 2. When the system is initially at equilibrium in the ferromagnetic phase, A scales as aR^n where $n \simeq \frac{1}{2}$ on the whole boundary and is almost independent of temperature r. On the

other hand, the temperature dependence of the coefficient a divides into two cases. For the second-order case,

$$a = a(r_c - r)^m \tag{9a}$$

where $r_c = -uS_c - vS_c^2$. a and m depend on the parameters u and v. This case is shown in figure 5 too (lines with $v = 50$ and 105.2758 ($< v_c$)). All lines there are parallel to each other with a slope of about $\frac{1}{2}$ following $A = aR^n$. The scaling of $A = a(r_c - r)^m R^n$ is fitted and shown in table 2. For the first order transition

$$a = \exp\left[a(r_f - r)^m\right]. \tag{9b}$$

a and m are functions of u and v. r_f is the first-order transition temperature in the r–u plane and is also a function of u and v[13], e.g. $r_f = 2.53$ for $u = -25.59$ and $v = 50$ (see table 1 in [13]). Figure 7 shows three lines of $A/\exp[a'(r_f - r)^m]$ versus R, both in logarithmic coordinates. They are all parallel to each other with a slope of $\frac{1}{2}$. The fitted values of m and a are listed in table 3.

Table 2. The fitted values of m and a (figure 5).

u	v	m	a
1	0	0.87	11.75
10	0	0.84	1.96
10	50	0.52	1.69
10	105.2758	0.49	1.39

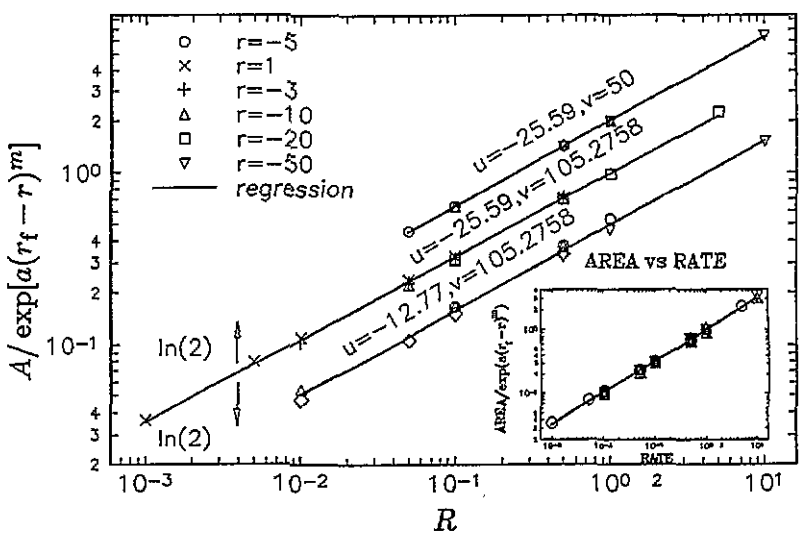

Figure 7. The lines of $\log\{A/\exp[a(r_f - r)^m]\}$ versus $\log R$ for hysteresis loops on the side of the first-order phase boundary in the ferromagnetic region. When the upper and lower lines are shifted ln 2 downwards and upwards, respectively, the three lines overlap into one as shown in the inset.

Table 3. Fitted values of m and a' (figure 7).

u	v	m	a'
−25.59	50	0.12	1.75
−25.59	105.28	0.18	1.22
−12.77	105.28	0.24	0.95

When the system is initially at equilibrium in the paramagnetic phase, magnetic field cycling may produce different scaling relations. When one goes towards the tricritical point near the phase boundary, the exponent might take the value of unity or even assume a different form of scaling relation. For the second-order transition, the hysteresis loop results from transition between 'up' and 'down' magnetization and $A = aR$, with an exponent of 1. This can be explained by dropping the space correlation and non-linear terms in equation (5) in the case of the paramagnetic phase. Hence, $dM/dt \simeq rM + H = rM + Rt$ and we obtain $M \simeq \int Rt \exp(-rt)\, dt \propto R$. The exceptional region is, however, very small and it could be taken as a crossover region of the exponent. It is left for further study to ascertain its exact range.

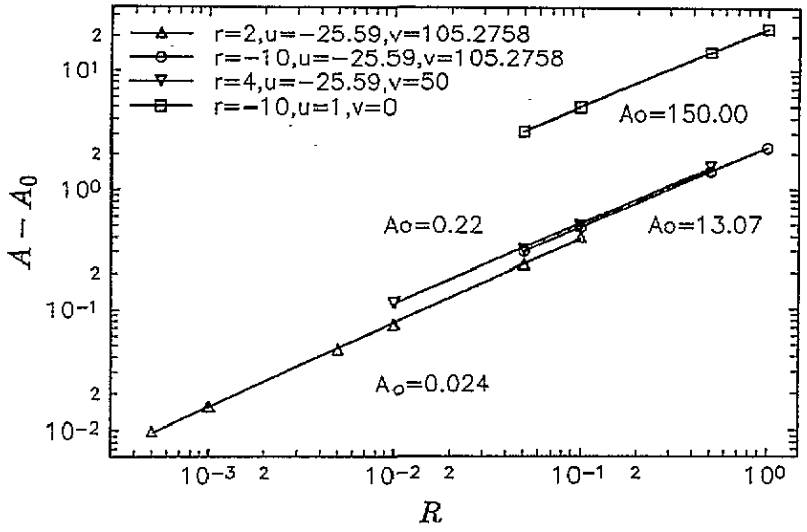

Figure 8. The $\log(A - A_0)$ versus R lines. The lowest line is the 'exceptional' case in the $(\Phi^2)^3$ theory (FTPD). All the other three lines are from the mean-field model.

For the first-order transition, double hysteresis loops develop. It is the field-theoretical paramagnetic double hysteresis (FTPDH). When $r = 2$, $u = -25.59$ and $v = 105.2758$, that is, away from the phase boundary $r_f = 1.28$ ($r > r_f$) and in the paramagnetic phase, the loop area scales as

$$A = A_0 + aR^n \tag{10}$$

(figure 8) with $n = 0.70$, where A_0 is the area of the static hysteresis loop solved from equation (5) by taking the time derivatives to be zero. It is noticed that the exponent is close to two thirds that of the mean-field model (see the next section). This is because thermal fluctuations in this theory are not strong enough to drive the system over the

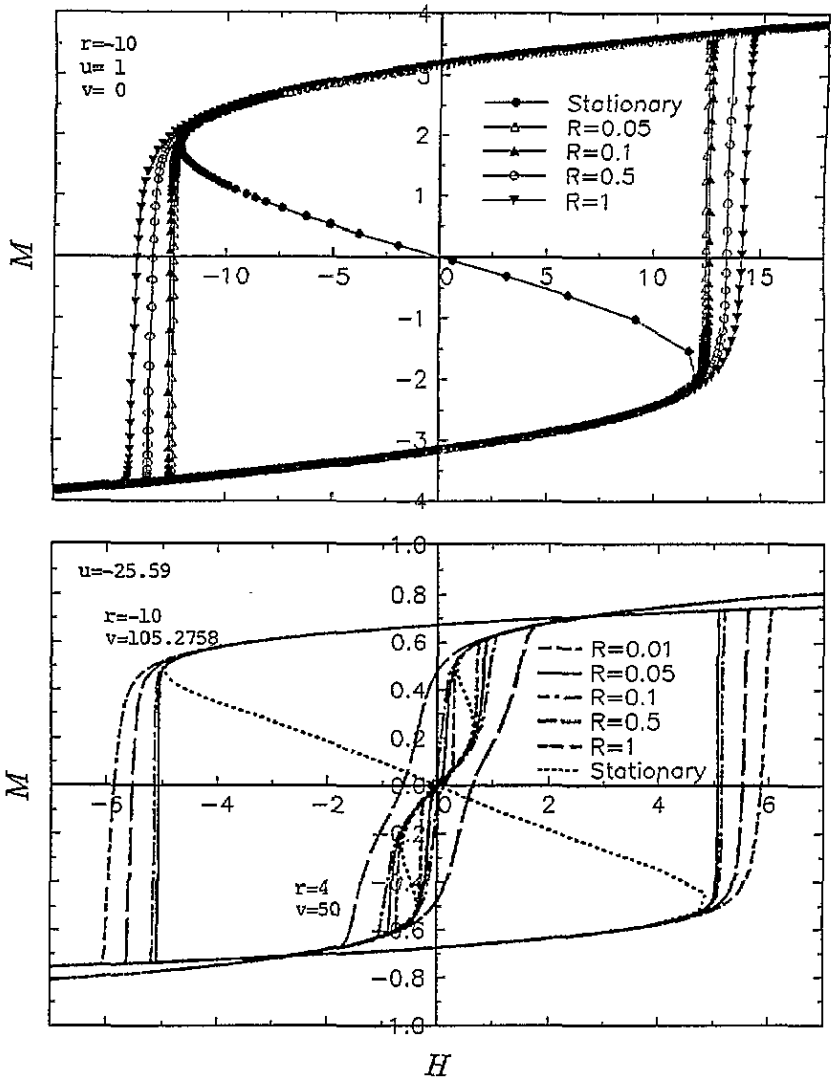

Figure 9. (a) Hysteresis loops as functions of field sweeping rate: $u = 1$, $v = 0$ and temperature $r = -10$. $R = 0$, 0.05, 0.1, 0.5 and 1 from the inside to the outside. (b) Hysteresis and double hysteresis loops as functions of field sweeping rate: $u = -25.59$, $v = 105.2758$, $r = -10$, for the outside loops and $u = -25.59$, $v = 50$ and $r = 4$, for the inside loops. The outside loops have four rates of 0.05, 0.1, 0.5 and 1; the inside loops also have four, 0.01, 0.05, 0.1 and 0.5, in which the first three result in double loops.

transition barrier so that the phase transition occurs only as the spinodal field is reached, just as in the mean-field model. The effect of thermal fluctuations on the phase transition will be reported later.

For the system in the ferromagnetic phase initially, the area of the hysteresis loop of the field-driven phase transition, either the FOPT or the second-order phase transition, scales as the $\frac{1}{2}$ power of the sweeping rate R. For the system in the paramagnetic phase initially, there are some exceptions; the exponent may be 1 near the tricritical point or may be about $\frac{2}{3}$. These cases show that the loop area does not scale in the same universal class.

4. The mean-field model

We now make a mean-field approximation to the two models. All spatial fluctuations of the order parameters are now ignored. the free energy is

$$F = \tfrac{1}{2}rM^2 + \tfrac{1}{4}uM^4 + \tfrac{1}{6}vM^6 - HM. \tag{11}$$

The equation of motion is

$$\mathrm{d}M/\mathrm{d}t = -\tfrac{1}{2}\left(rM + uM^3 + vM^5 - H\right) \tag{12}$$

where time is also in units of $(2\Gamma)^{-1}$. Hysteresis loops and double hysteresis loops are shown in figure 9(a) for $v = 0$, and in figure 9(b) for $v \neq 0$. The stationary curve $H = rM + uM^2 + vM^5 - H$ is also presented for comparison. Transformation occurs only when $H > H_c$, the spinodal field, since there is no fluctuation. The area of the loops scales as $A = A_0 + aR^n$, where A_0 is the area between H_c and $-H_c$. The scaling lines are also shown in figure 8 together with that of FTPDH. The lines are parallel to each other with a slope (the exponent) $n = 0.67$, very close to $n = 0.70$ for FTPDH. It follows that both the mean-field and the FTPDH models belong to a class different from the theoretical ferromagnetic model, although FTDPH has already taken spatial fluctuation into account.

5. Discussion

The time-dependent Ginzburg–Landau theory is a prototype formulation applied successfully in the dynamics of critical phenomena and FOPT. On the basis of this theory we investigate the hysteresis of the $(\Phi^2)^2$, $(\Phi^2)^3$ and mean-field models in a linear driving mode. When the systems are initially at equilibrium in the ferromagnetic phase, the loop area A obeys a power law, $aR^{1/2}$. The exponent $\frac{1}{2}$ is independent of temperature r and parameter u or v. However, the scaling of the coefficient a with temperature has two forms as shown by equation (9). For the mean-field model and FTPDH, there is a non-zero static hysteresis and the loop area scales as shown by equation (10) with an exponent close to $\frac{2}{3}$.

The field-theoretical models possess continuous symmetry and concern homogeneous nucleation. On comparison of the scaling of the dissipation, $aR^{1/2}$, with the scaling of the characteristic length L in equation (6), $L \propto t^{1/2}$, it is readily seen that the former is not as general as the latter as shown in figure 6 when exceptions such as 1 and $\frac{2}{3}$ are considered. However, theoretical investigation does give a scaling expression and value of exponent compatible with preliminary experimental evidence [14–19].

References

[1] Homma H and Clarke R 1984 *Phys. Rev. Lett.* **52** 629–32
[2] Katano S and Iizumi M 1984 *Phys. Rev. Lett.* **52** 835–8
[3] Tringides M C, Wu P K and Legally M G 1987 *Phys. Rev. Lett.* **59** 315–8
[4] Mazenko F 1991 *Phys. Rev.* B **43** 8204–10
[5] Binder K and Stauffer D 1974 *Phys. Rev. Lett.* **33** 1006–9
[6] Lifshitz I M and Slyozov V V 1961 *J. Phys. Chem. Solids* **19** 35
[7] Binder K 1977 *Phys. Rev.* B **15** 4425–47
[8] Furukawa H 1979 *Phys. Rev. Lett.* **43** 136
[9] Lifshitz I M 1962 *Zh. Eksp. Theor. Fiz.* **42** 1354 (Engl. Transl. 1962 *Sov. Phys.–JETP* **15** 939)

[10] Allen S M and Cahn J W 1979 *Acta Metall.* **27** 1085; 1977 *J. Physique* **38** C7 57
[11] Otsuka K and Shimizu K 1986 *Int. Met. Rev.* **31** 93, and references therein
[12] Rao M, Krishnammurthy H R and Pandit R 1990 *Phys. Rev.* B **42** 856
[13] Rao M and Pandit R 1991 *Phys. Rev.* B **43** 3373
[14] Zhang J X, Chen M H, Liu D M, Siu G G and Stokes M J 1989 *J. Phys.: Condens. Matter* **1** 9717–28
[15] Zeng W G, Lin H Q, Zhang J X and Siu G G 1990 *J. Phys.: Condens. Matter* **2** 9531–9
[16] Zeng W G, Zhang J X and Siu G G 1991 *J. Phys.: Condens. Matter* **3** 4783–95
[17] Zeng W G and Siu G G 1993 *J. Phys.: Condens. Matter* **5** 6461–8
[18] Zhang J X and Zeng W G 1986 *Acta Sci. Naturalium Uni. Sunyatseni* **4** 21–30
[19] Lin Z C, Liang K F, Zeng W G and Zhang J X 1989 *Internal Friction and Ultrasonic Attenuation* ed T S Ké and L D Zhang (Beijing: Atomic Energy Press of China) pp 87–8
[20] Mazenko G F and Zanneti M 1985 *Phys. Rev.* B **32** 4565
[21] Huse D A and Fisher D S 1986 *Phys. Rev. Lett.* **57** 2203
Parshin D A 1992 *Phys. Rev.* B **46** 761
[22] Bray A J and Humayun K 1990 *J. Phys. A: Math. Gen.* **23** 5897 and references therein
[23] Liu F and Mazenko G F 1992 *Phys. Rev.* B **45** 6989
Mazenko G F 1990 *Phys. Rev.* B **42** 4487
[24] Lawrie I D 1985 *Nucl. Phys.* B **257** 29